Noboru Takigawa · Kouhei Washiyama

Fundamentals of Nuclear Physics

Springer

Fundamentals of Nuclear Physics

Noboru Takigawa · Kouhei Washiyama

Fundamentals of Nuclear Physics

Springer

Noboru Takigawa
Department of Physics
Graduate School of Science
Tohoku University
Sendai
Japan

Kouhei Washiyama
Center for Computational Sciences
University of Tsukuba
Tsukuba, Ibaraki
Japan

ISBN 978-4-431-55377-9 ISBN 978-4-431-55378-6 (eBook)
DOI 10.1007/978-4-431-55378-6

Library of Congress Control Number: 2016958483

Translation from the Japanese language edition: *Genshikaku Butsurigaku* by Noboru Takigawa, © Asakura Publishing Company, Ltd. 2013. All rights reserved.

Printed on acid-free paper

This Springer imprint is published by Springer Nature
The registered company is Springer Japan KK
The registered company address is: Chiyoda First Bldg. East, 3-8-1 Nishi-Kanda, Chiyoda-ku, Tokyo 101-0065, Japan

To Noriko, Akiko, Tsuyoshi
and to our parents.

Preface

This book provides an introduction to nuclear physics. Research in nuclear physics covers a wide variety of subjects, and one can list many key words: nuclear structure and reactions of stable and unstable nuclei, fission and decay of a nucleus, extreme states such as the limits of existence and high-spin states, properties at high temperature and high density, hypernuclei, neutron stars, and nucleosynthesis, among others. All of these are the subjects of nuclear physics. In addition to these rather static properties, nuclear reactions such as heavy-ion collisions introduce new aspects of research, i.e., dynamical properties of nuclei or reaction mechanisms, such as heavy-ion fusion reactions, dissipation phenomena and liquid–gas phase transition. Many of these phenomena can be understood from the point of view that a nucleus is a quantum many-body system of nucleons stabilized by nuclear force. On the other hand, phenomena at higher energies, driven by, e.g., high-energy heavy-ion collisions, require a different approach: the approach based on the quantum chromodynamics (QCD). The study of quark–gluon plasma and of the QCD phase diagram is representative and forms a large stream of current nuclear physics.

In this book, we largely restrict our subjects and describe basic features of nuclear structure and of nuclear decays. β-decay and most excitation motions are left to other books. Also, nuclear reactions and current subjects such as physics of unstable nuclei, hypernuclei, and nuclear physics based on QCD are untouched except for occasional very brief references. Even with these limitations, we could only briefly mention recent developments. However, we have tried to convey part of them through columns on the QCD phase diagram of nuclear matter, superheavy elements, superdeformed states, and overview of the synthesis of elements. We hope that together with the main text they help readers to grasp our current knowledge of the nucleus and some recent research trends in nuclear physics. By restricting the subjects, our aim was to contain many experimental data of basic nuclear properties or suitable illustrations and explain the main structural features of nuclei in some detail. This will be useful because most of the phenomena listed in the first paragraph, but omitted from the book, are intimately related to those basic properties. We also have attempted to explain how the nuclear model has

developed from the original phenomenological level of a shell model to the modern understanding based on a many-body theory such as the Hartree–Fock calculations. We also have described nuclear force, the basis of nuclear physics, in some detail. We sometimes introduce semi-classical approximation to the original quantum mechanical formalism. We hope that it helps the readers to intuitively grasp the underlying physics of complicated nuclear phenomena.

In writing the book our intention was to create not only a good introduction to nuclear physics, but also a good reference book for physicists to learn the application of quantum mechanics and mathematics. Toward that aim, in addition to describing the basic phenomena of a nucleus, we attempted to convey how the basic subjects of modern physics such as quantum mechanics, statistical physics, mathematics for physics, e.g., complex integrals, are used to describe or interpret various phenomena of nucleus. We also considered the standard level of knowledge of junior and senior students, and gave a detailed description to enable them to derive each equation. Finally, we added the appendix to prove a number of important formulae in the main text and to show some fundamental formulae.

The contents of the book are based on the lectures that one of the authors, N.T., has delivered at Tohoku University, Sendai, Japan, for a long time to junior and senior students in the undergraduate physics course and also to beginning graduate students. We have included as sidebars some additional material that was presented in the class in order to keep the atmosphere of the lecture. Many textbooks and original papers and figures therein have helped in preparing the lectures and this book. Several of the figures are taken from them. Using this opportunity, we wish to thank the authors. The papers cited at various places are not at all complete. Moreover, it does not mean that they are necessarily the representative papers on each citation. Nevertheless, we hope that they can help readers to do further study. This book is an English translation of the Japanese edition, which one of the authors, N.T., published in 2013. The appendix contains the errata to the original Japanese edition.

We would like to thank Akif Baha Balantekin for many useful comments for the writing of this English edition. We thank D.M. Brink, A.B. Balantekin, N. Rowley, F. Michel, S.Y. Lee, P. Fröbrich, S. Landowne, K. McVoy, W.A. Friedman, G.F. Bertsch, A. Brown, H. Weidenmüller, H. Friedrich, H. Esbensen, M.S. Hussein, L.F. Canto, C. Bertulani, P.R.S. Gomes, D. Hinde, M. Dasgupta, G. Pollarolo, A. Bonasera, M. Di Toro, C. Spitaleri, C. Rolfs, I. Thompson, S. Ayik, K. Hara, Y. Abe, H. Sagawa, A. Iwamoto, T. Tazawa, M. Ohta, J. Kasagi, and many other colleagues and friends around the world; and K. Hagino and A. Ono in the Nuclear Theory Group of Tohoku University, Sendai, for useful discussions. We are grateful to students of Tohoku University, especially foreign students, for stimulating us to write this English book. We would like to thank F. Minato, S. Yusa, S. Iwasaki and his wife, H. Tamura, and H. Koura for preparing figures, and K. Morita, T. Hirano, Y. Aritomo, T. Kajino, and Y. Motizuki in preparing the columns; and P. Möller, T. Wada, K. Matsuyanagi, T. Tamae, and K. Kato for kindly reading sections of the Japanese edition and making many helpful suggestions. We also thank all the mentors and collaborators who provided

us opportunities to work in their institutions. We are grateful to H. Niko and R. Takizawa for their help as the editors of this English version. Above all N.T. would like to thank his wife, Noriko, and his family for their support over the years.

Sendai, Japan
September 2016

Noboru Takigawa
Kouhei Washiyama

Contents

1 Introduction 1
1.1 The Constituents and Basic Structure of Atomic Nuclei 1
1.2 Properties of Particles Relevant to Nuclear Physics 2
1.3 The Role of Various Forces 6
1.4 Useful Physical Quantities 7
1.5 Species of Nuclei 8
1.6 Column: QCD Phase Diagram of Nuclear Matter 11
References 12

2 Bulk Properties of Nuclei 13
2.1 Nuclear Sizes 13
2.1.1 Rutherford Scattering 13
2.1.2 Electron Scattering 17
2.1.3 Mass Distribution 25
2.2 Number Density and Fermi Momentum of Nucleons 28
2.2.1 Number Density of Nucleons 28
2.2.2 Fermi Momentum: Fermi-Gas Model, Thomas–Fermi Approximation 28
2.3 Nuclear Masses 31
2.3.1 The Binding Energies: Experimental Data and Characteristics 32
2.3.2 The Semi-empirical Mass Formula (The Weizsäcker–Bethe Mass Formula)—The Liquid-Drop Model 42
2.3.3 Applications of the Mass Formula (1): The Stability Line, the Heisenberg Valley 43
2.3.4 Applications of the Mass Formula (2): Stability with Respect to Fission 46
2.3.5 Application to Nuclear Power Generation 57
2.3.6 Fission Isomers 60
References 64

3 The Nuclear Force and Two-Body Systems 65
3.1 The Fundamentals of Nuclear Force 65
3.1.1 The Range of Forces—A Simple Estimate by the Uncertainty Principle 65
3.1.2 The Radial Dependence 66
3.1.3 The State Dependence of Nuclear Force 67
3.2 The General Structure of Nuclear Force 71
3.2.1 Static Potentials (Velocity-Independent Potentials) 71
3.2.2 Velocity-Dependent Potentials 73
3.3 The Properties of Deuteron and the Nuclear Force 74
3.3.1 The Effect of Tensor Force: The Wave Function in the Spin–Isospin Space 74
3.3.2 The Radial Wave Function: Estimate of the Magnitude of the Force Between Proton and Neutron 77
3.4 Nucleon–Nucleon Scattering 78
3.4.1 Low-Energy Scattering: Effective Range Theory 78
3.4.2 High-Energy Scattering: Exchange Force 81
3.4.3 High-Energy Scattering: Repulsive Core 83
3.4.4 Spin Polarization Experiments 85
3.5 Microscopic Considerations: Meson Theory, QCD 85
3.6 Phenomenological Potential with High Accuracy: Realistic Potential 88
3.6.1 Hamada–Johnston Potential 89
3.6.2 Reid Potential 91
3.7 Summary of the Nuclear Force in the Free Space 91
3.8 Effective Interaction Inside Nucleus 92
3.8.1 *G*-Matrix 92
3.8.2 Phenomenological Effective Interaction 94
References 96

4 Interaction with Electromagnetic Field: Electromagnetic Moments 97
4.1 Hamiltonian of the Electromagnetic Interaction and Electromagnetic Multipole Moments 97
4.1.1 Operators for the Dipole and Quadrupole Moments 98
4.1.2 Various Corrections 100
4.1.3 Measurement of the Magnetic Moment: Hyperfine Structure 100
4.2 Electromagnetic Multipole Operators 102
4.3 Properties of the Electromagnetic Multipole Operators 103
4.3.1 Parity, Tensor Property and Selection Rule 103
4.3.2 Definition of the Electromagnetic Moments 104
References 106

5 Shell Structure 107
5.1 Magic Numbers 107
5.2 Explanation of the Magic Numbers by Mean-Field Theory 109
5.2.1 The Mean Field 109
5.2.2 Energy Levels for the Infinite Square-Well Potential 110
5.2.3 The Harmonic Oscillator Model 111
5.2.4 The Magic Numbers in the Static Potential Due to Short Range Force 112
5.2.5 Spin–Orbit Interaction 114
5.3 The Spin and Parity of the Ground and Low-Lying States of Doubly-Magic ± 1 Nuclei 117
5.4 The Magnetic Dipole Moment in the Ground State of Odd Nuclei: Single Particle Model 119
5.4.1 The Schmidt Lines 120
5.4.2 Configuration Mixing and Core Polarization 121
5.4.3 [Addendum] The Anomalous Magnetic Moments of Nucleons in the Quark Model 123
5.5 Mass Number Dependence of the Level Spacing $\hbar\omega$ 124
5.6 The Magnitude and Origin of Spin–Orbit Interaction 125
5.7 Difference Between the Potentials for Protons and for Neutrons: Lane Potential 125
5.8 The Spin and Parity of Low-Lying States of Doubly-Magic ± 2 Nuclei and the Pairing Correlation 127
5.8.1 The Spin and Parity of the Ground and Low Excited States of $^{210}_{82}$Pb 127
5.8.2 The Effect of δ-Type Residual Interaction: Pairing Correlation 128
5.9 Column: Superheavy Elements (SHE) 130
References 133

6 Microscopic Mean-Field Theory (Hartree–Fock Theory) 135
6.1 Hartree–Fock Equation 135
6.1.1 Equivalent Local Potential, Effective Mass 136
6.1.2 Nuclear Matter and Local Density Approximation 137
6.1.3 Saturation Property in the Well-Behaved Potential, Constraint to the Exchange Property 140
6.2 Skyrme Hartree–Fock Calculations for Finite Nuclei 141
6.2.1 Skyrme Force 141
6.2.2 Skyrme Hartree–Fock Equation 143
6.2.3 Energy Density and Determination of Parameters 144
6.2.4 Comparison with the Experimental Data 147
6.2.5 The Equation of State, Saturation, Spinodal Line, Surface Thickness 148
6.2.6 Beyond the Hartree–Fock Calculations: Nucleon–Vibration Coupling; ω-Mass 154

6.3 Relativistic Mean-Field Theory ($\sigma\omega\rho$ Model) . . . 155
6.3.1 Lagrangian . . . 156
6.3.2 Field Equations . . . 157
6.3.3 The Mean-Field Theory . . . 158
6.3.4 Prologue to How to Solve the Mean-Field Equations . . . 158
6.3.5 Non-relativistic Approximation and the Spin–Orbit Coupling . . . 160
6.3.6 Parameter Sets . . . 161
6.4 Pairing Correlation . . . 162
6.4.1 Overview . . . 162
6.4.2 Multipole Expansion of the Pairing Correlation, Monopole Pairing Correlation Model and Quasi-Spin Formalism . . . 163
6.4.3 BCS Theory . . . 164
6.4.4 The Magnitude of the Gap Parameter . . . 168
6.4.5 The Coherence Length . . . 169
References . . . 170

7 The Shapes of Nuclei . . . 171
7.1 The Observables Relevant to the Nuclear Shape: Multipole Moments and the Excitation Spectrum . . . 171
7.2 Deformation Parameters . . . 174
7.3 The Deformed Shell Model . . . 177
7.4 Nucleon Energy Levels in a Deformed One-Body Field: Nilsson Levels . . . 180
7.5 The Spin and Parity of the Ground State of Deformed Odd Nuclei . . . 182
7.6 Theoretical Prediction of Nuclear Shape . . . 182
7.6.1 The Strutinsky Method: Macroscopic–Microscopic Method . . . 182
7.6.2 Constrained Hartree–Fock Calculations . . . 184
7.7 Column: Superdeformed States . . . 187
References . . . 188

8 Nuclear Decay and Radioactivity . . . 191
8.1 Alpha Decay . . . 191
8.1.1 Decay Width . . . 192
8.1.2 The Geiger–Nuttal Rule . . . 200
8.2 Fission . . . 200
8.3 Electromagnetic Transitions . . . 203
8.3.1 Multipole Transition, Reduced Transition Probability . . . 203
8.3.2 General Consideration of the Selection Rule and the Magnitude . . . 205
8.3.3 Single-Particle Model Estimate: Weisskopf Units and Experimental Values . . . 206

8.3.4 Connection Between Electromagnetic Transitions and the Shapes and Collective Motions of Nuclei 209
References 212

9 Synthesis of Elements 215
9.1 The Astrophysical S-Factor and Gamow Factor 215
9.2 Gamow Peak 217
9.3 Neutron Capture Cross Section 218
9.4 Synthesis of Heavy Elements: S-Process and R-Process 219
9.5 Column: Overview of the Synthesis of Elements 220
References 221

Appendix A: Important Formulae and Their Derivation 223

Index 261

Chapter 1
Introduction

Abstract It would be useful to have an overview of some fundamental aspects of nuclei before discussing each subject in detail. In this connection, we briefly describe in this chapter the constituents and basic structure of atomic nuclei, properties of particles which are closely related to nuclear physics, the role of the four fundamental forces in nature in nuclear physics, nuclear species, the abundance of elements and the phase diagram of nuclear matter.

1.1 The Constituents and Basic Structure of Atomic Nuclei

The atomic nuclei are self-bound many-body systems of protons (p) and neutrons (n) by strong interaction. Although other baryons such as $\Delta(1232)$ are also contained, their amounts are small. For example, the percentage of $\Delta(1232)\Delta(1232)$ contained in the lightest nucleus deuteron (d) is about 1%. π-mesons in virtual states mediate the interaction between the constituent particles and affect the electromagnetic properties of protons and neutrons. Furthermore, each proton and neutron is also a composite particle consisting of three quarks. The other hadrons also consist of quarks. One can therefore take also the view that atomic nuclei are many-body systems of quarks.

The picture of nuclei and of nuclear phenomena, hence the appropriate way to describe them, depend on the object and method of observation and the related energy scale, and lead to various models for nuclei. This book restricts to low-energy phenomena and discusses the nuclear structure and properties primarily from the point of view that nuclei are many-body systems of protons and neutrons. The governing law is quantum mechanics. This contrasts to quantum chromodynamics for high-energy phenomena. Among various quantum many-body systems, nuclei have characteristics that the number of constituents is small and also that the leading forces are strong interactions.

Each nucleus is represented, for example, as ${}^{16}_{8}\mathrm{O}$. O is the symbol of the chemical element. It represents oxygen in this example, hence the number of protons is 8. This number is called the atomic number, and is given at the left lower side. It is often omitted, because it has a one to one correspondence to the symbol of element. The number at the left upper side is called mass number and is given by the sum

N. Takigawa and K. Washiyama, *Fundamentals of Nuclear Physics*,
DOI 10.1007/978-4-431-55378-6_1

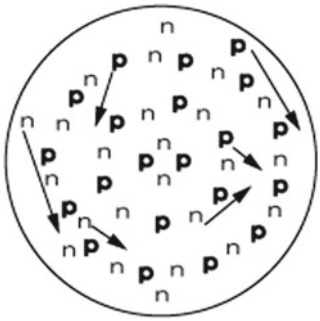

Fig. 1.1 Conceptual illustration of nuclear structure: example of $^{45}_{21}$Sc

of the atomic number and the neutron number. They are denoted by A, Z and N, respectively, and $A = Z + N$.

Figure 1.1 is a conceptual illustration of nuclear structure exemplified by $^{45}_{21}$Sc. The enclosing circle has been drawn to indicate the finiteness of the nuclear size. In reality, it is absent, because nuclei are not given by any external boundary conditions, but are self-bound systems. The arrows indicate that protons p and neutrons n inside a nucleus are not fixed at lattice points like atoms in solids, but are moving around with finite velocities. We learn later that nuclei behave like either liquid or gas depending on the observables or phenomena we are interested in.

1.2 Properties of Particles Relevant to Nuclear Physics

Table 1.1 gives the properties of particles which are closely related to this book. As the table shows, proton and neutron resemble each other in many properties such as the mass and the spin except for electric properties, and are jointly called *nucleons*. In order to distinguish them, one introduces the concept of *isospin space* related to charge, and considers proton and neutron to be two different states in the isospin space. The operators and states in the isospin space obey the same law as that of angular momentum, and are called isospin operators and isospin states, respectively.

Nucleon has two states in the isospin space. Similarly to the spin operators for electron $\hat{\mathbf{s}}$, one therefore introduces the isospin operators $\hat{\mathbf{t}}$ by

$$\hat{t}_x = \frac{1}{2}\begin{pmatrix} 0 & 1 \\ 1 & 0 \end{pmatrix}, \quad \hat{t}_y = \frac{1}{2}\begin{pmatrix} 0 & -\mathrm{i} \\ \mathrm{i} & 0 \end{pmatrix}, \quad \hat{t}_z = \frac{1}{2}\begin{pmatrix} 1 & 0 \\ 0 & -1 \end{pmatrix}, \tag{1.1}$$

and, analogously to the Pauli spin operators $\hat{\boldsymbol{\sigma}}$, $\hat{\boldsymbol{\tau}} = 2\hat{\mathbf{t}}$ by

$$\hat{\tau}_x = \begin{pmatrix} 0 & 1 \\ 1 & 0 \end{pmatrix}, \quad \hat{\tau}_y = \begin{pmatrix} 0 & -\mathrm{i} \\ \mathrm{i} & 0 \end{pmatrix}, \quad \hat{\tau}_z = \begin{pmatrix} 1 & 0 \\ 0 & -1 \end{pmatrix}, \tag{1.2}$$

Table 1.1 Properties of particles relevant to nuclear physics. I: isospin, S: strangeness, R_c: radius of charge distribution, μ: magnetic dipole moment, m in the magneton $e\hbar/2mc$ is m_e for electron, m_μ for μ particle, m_p for proton and neutron, and m_p for Λ and Σ particles. The number represents the mean value if error is not given. The lifetime of proton depends on methods. The mass of ν is from the decay of tritium. The lifetime of ν is from nuclear reactor with m_{ν_e} in units of eV. The quark structure for $\rho^{\pm,0}$ is the same as that for $\pi^{\pm,0}$. Taken from [1]

Name	I	I_3	J^π	S	mc^2 (MeV)	R_c (fm)	μ ($\frac{e\hbar}{2mc}$)	τ(mean life) (s)	Quark model
p	$\frac{1}{2}$	$-\frac{1}{2}$	$\frac{1}{2}^+$	0	938.3	0.88 ± 0.01	2.79	$>1.9 \times 10^{29}$ y	uud
n	$\frac{1}{2}$	$\frac{1}{2}$	$\frac{1}{2}^+$	0	939.6	0.34[a]	−1.91	885.7 ± 0.8	udd
γ			1^-		$<6 \times 10^{-23}$			stable	
$W^\pm$			1		80.4×10^3			3.1×10^{-25}	
Z^0			1		91.2×10^3			2.7×10^{-25}	
ν_e			$\frac{1}{2}$		$<2 \times 10^{-6}$		[b]	$>300 m_{\nu_e}$	
e^-			$\frac{1}{2}$		0.511		1.00	$>4.6 \times 10^{26}$ y	
μ^-			$\frac{1}{2}$		105.7		1.00	2.2×10^{-6}	
π^+	1	1	0^-	0	139.6			2.6×10^{-8}	$u\bar{d}$
π^-	1	−1	0^-	0	139.6			2.6×10^{-8}	$d\bar{u}$
π^0	1	0	0^-	0	135.0			0.84×10^{-16}	$\frac{1}{\sqrt{2}}(u\bar{u}-d\bar{d})$
$\rho^{\pm,0}$	1		1^-		775.5			4.5×10^{-24}	$(u\bar{d}, d\bar{u})$
ω	0		1^-		782.7			7.9×10^{-23}	[c]
K^+	$\frac{1}{2}$	$\frac{1}{2}$	0^-	1	493.7			1.24×10^{-8}	$u\bar{s}$
K^-	$\frac{1}{2}$	$-\frac{1}{2}$	0^-	−1	493.7			1.24×10^{-8}	$s\bar{u}$
K^0	$\frac{1}{2}$	$-\frac{1}{2}$	0^-	1	497.6				$d\,\bar{s}$
$\bar{K}^0$	$\frac{1}{2}$	$\frac{1}{2}$	0^-	−1	497.6				$s\,\bar{d}$
Λ	0	0	$\frac{1}{2}^+$	−1	1115.7		−0.61	2.63×10^{-10}	uds
Σ^+	1	1	$\frac{1}{2}^+$	−1	1189.4		2.46	0.80×10^{-10}	uus
Σ^0	1	0	$\frac{1}{2}^+$	−1	1192.6			$(7.4 \pm 0.7) \times 10^{-20}$	uds
Σ^-	1	−1	$\frac{1}{2}^+$	−1	1197.4			1.5×10^{-10}	dds
Ξ^0	$\frac{1}{2}$	$\frac{1}{2}$	$\frac{1}{2}^+$	−2	1314.8			2.9×10^{-10}	uss
Ξ^-	$\frac{1}{2}$	$-\frac{1}{2}$	$\frac{1}{2}^+$	−2	1321.3			1.6×10^{-10}	dss
Δ	$\frac{3}{2}$		$\frac{3}{2}^+$	0	~ 1232			$\sim 6 \times 10^{-24}$	[d]

[a] The mean square charge radius of neutron is $\langle r_n^2 \rangle = -0.1161 \pm 0.0022\,\text{fm}^2$
[b] $\mu_\nu < 0.54 \times 10^{-10} \mu_B$
[c] $c_1(u\bar{u}+d\bar{d})+c_2 s\bar{s}$
[d] Δ^{++} =uuu, Δ^+ =uud, Δ^0 =udd, Δ^- =ddd

and considers proton and neutron to be simultaneous eigenstates of $\hat{\mathbf{t}}^2$ and $\hat{t}_z$ in such a way that[1]

$$|\mathrm{n}\rangle = \left|\frac{1}{2}\ \frac{1}{2}\right\rangle = \begin{pmatrix}1\\0\end{pmatrix}\ , \quad |\mathrm{p}\rangle = \left|\frac{1}{2}\ -\frac{1}{2}\right\rangle = \begin{pmatrix}0\\1\end{pmatrix}\ . \tag{1.3}$$

As Table 1.1 shows, the isospin is one of the important quantum numbers to specify the property of each particle. Its magnitude is assigned to be I when there exist $2I+1$ particles which have common properties for all aspects such as the mass and spin but the electric charge. For example, the isospin of π-mesons is 1, since there exist three particles which differ only in the electric charge. In nuclei, the isospin quantum number of each state and the symmetry concerning the isospin play important roles reflecting the symmetry properties of nuclear force in the isospin space.

If a particle is a structureless fermion, one can deduce from the Dirac equation that its magnetic dipole moment, which is often simply called magnetic moment, is given by $\mu = e\hbar/2mc$, where m is the mass of the particle. In fact, the magnetic moment of an electron is 1 in units of the *Bohr magneton* $\mu_\mathrm{B} = e\hbar/2m_\mathrm{e}c$.[2] However, Table 1.1 shows that the magnetic moment of a proton significantly deviates from the *nuclear magneton* $\mu_N = e\hbar/2m_\mathrm{p}c$. Also, the magnetic moment of a neutron is not zero, but is nearly comparable in magnitude and opposite in sign to that of a proton. They are called *anomalous magnetic moments* and imply that both the proton and the neutron are composite particles with intrinsic structure.[3]

Exercise 1.1 Derive the approximate equation for two large components φ in the four-component spinor ψ starting from the Dirac equation in the presence of electromagnetic fields and assuming that the velocity v of the particle is much smaller than the speed of light in vacuum c, i.e., $v \ll c$, and show that the term which describes the interaction with the magnetic field in the effective Hamiltonian is given by $H = -\frac{e\hbar}{2mc}\boldsymbol{\sigma}\cdot\mathbf{B}$, where $\mathbf{B}$ is the magnetic field. One can thus prove that the magnetic moment of a Dirac particle is given by $e\hbar/2mc$.

The fact that both proton and neutron are not point particles, but have intrinsic structure, can be seen also directly from the data of charge distribution. The radius of the charge distribution of a proton is about 1 fm.[4]

---

[1] There exists an alternative definition, where proton and neutron are inverted such that $|\mathrm{p}\rangle = |\frac{1}{2}\ \frac{1}{2}\rangle$, $|\mathrm{n}\rangle = |\frac{1}{2}\ -\frac{1}{2}\rangle$. Since $N \geq Z$ for most stable nuclei, we adopt the Definition (1.3) in this book.

[2] Precisely speaking, the experimental value of the magnetic moment of an electron is larger than the prediction of the Dirac theory by about 0.1%, and can be explained by quantum electrodynamics.

[3] It is Otto Stern who experimentally determined the magnetic moment of a proton for the first time. There remains an episode that Pauli visited Stern while he was conducting the experiment and denied the significance of the experiment based on the Dirac theory. Despite the criticism, Stern continued his experiment, and discovered the anomalous magnetic moment of a proton, and consequently was awarded the Nobel Prize in Physics in 1943.

[4] Recent experiments of the scattering of high-energy electrons, and also of polarized electrons, are shedding new lights on the intrinsic structure of nucleons. For example, it is getting uncovered that the electric and magnetic charge distributions are different.

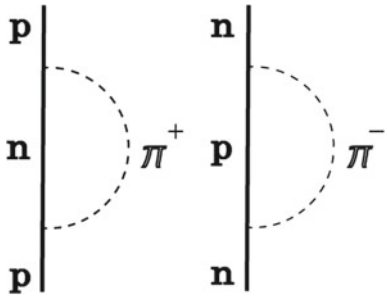

Fig. 1.2 A physical nucleon dressed with a virtual π-meson cloud

The anomalous magnetic moments of nucleons can be understood by either the meson theory or the quark model. The latter will be explained in Sect. 5.4.3. Here, we learn the former.

Let us assume that the proton observed in experiments is a superposition of a bare proton as a structureless Dirac particle and a bare neutron as a Dirac particle surrounded by a virtual π^+-meson (the left part of Fig. 1.2),

$$|\mathrm{p}\uparrow) = \sqrt{1-C_\mathrm{p}}|\mathrm{p}\uparrow\rangle + \sqrt{C_\mathrm{p}}|(\mathrm{n}\times\pi^+)\uparrow\rangle\ . \tag{1.4}$$

Since the π-meson is a pseudoscalar particle, the orbit of the π-meson around the neutron is p-orbit. Corresponding to Eq. (1.4), the magnetic moment of a proton will be given by

$$\mu_\mathrm{p} = (1-C_\mathrm{p})\mu_N + C_\mathrm{p}\frac{e\hbar}{2m_\pi c}\ . \tag{1.5}$$

The first and the second terms on the right-hand side represent the contribution of the interaction of the electromagnetic field with a bare proton and with π-meson, respectively. Because of the difference between the masses of a nucleon and a π-meson, one can explain the anomalous magnetic moment of a proton by assuming the admixture of the (neutron$\times\pi^+$-meson)-component in a proton to be about 30%.

Similarly, if one assumes that a neutron is not a genuine Dirac particle, but contains the component, where π^--meson is moving around a proton as a Dirac particle, by C_n in proportion (the right part of Fig. 1.2), one obtains

$$\mu_\mathrm{n} = C_\mathrm{n}\left(\mu_N - \frac{e\hbar}{2m_\pi c}\right) \tag{1.6}$$

for the magnetic moment of a neutron. Assuming $C_\mathrm{p} = C_\mathrm{n}$, one obtains

$$\mu_\mathrm{p} + \mu_\mathrm{n} = \mu_N\ . \tag{1.7}$$

This agrees well with the experimental data $(\mu_\mathrm{p}+\mu_\mathrm{n})_\mathrm{exp} \sim 0.88\mu_N$.

1.3 The Role of Various Forces

It is known that four types of forces exist in nature. In this section, we briefly survey the role of four forces in nuclear physics.

The strong interaction is principally responsible for the stability and the structure of nuclei. *The electromagnetic interaction* provides a powerful probe of nuclear structure through the electron scattering from nuclei as well as electromagnetic transitions and moments thanks to its well understood nature and the weakness of the force. Furthermore, it governs the lifetime of excited states of nuclei through the electromagnetic transition by γ-ray emission. *The weak interaction* governs the stability of nuclei through $\beta^{\pm}$-decay. The representative example is the beta decay of neutron (Fig. 1.3), which is given by

$$\mathrm{n} \rightarrow \mathrm{p} + \mathrm{e}^{-} + \bar{\nu}_{\mathrm{e}} \ . \tag{1.8}$$

As shown in Table 1.1, the mean life of the neutron in free space is $\tau \sim 14.8$ min, and the corresponding half-life is $T_{1/2} \sim 10.2$ min. The weak interaction plays an important role also in the synthesis of elements beyond Fe.

Exercise 1.2 Explain the reason why the third particle besides the proton and the electron is needed in the final state of the β-decay of the neutron. Also, discuss the properties of that particle.

All of the strong, the electromagnetic and the weak interactions are relevant to the decay of nuclei. Though there are a large variety of decays, the time scale of the lifetime associated with them is of the order of 10^{-21} s, 1 ps $= 10^{-12}$ s, and 1 min, respectively, reflecting the difference among their strengths.

The gravitational force plays almost no role in the structure of nuclei. However, it plays a crucial role in the synthesis of elements. Also, as we learn later, although there exists no stable nucleus of dineutrons, there exist *neutron stars* because of the gravitational force.

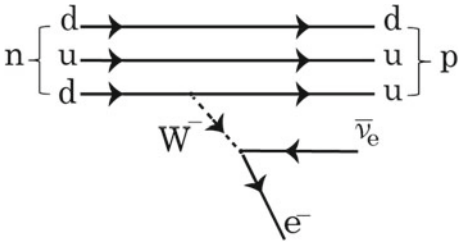

Fig. 1.3 The β-decay of a neutron

1.4 Useful Physical Quantities

It is sometimes worth making order-of-magnitude estimates of various physical quantities. In that connection. it is useful to remember the following approximate values related to the fundamental physical constants c (the speed of light in vacuum), $\hbar$ (the Planck constant divided by 2π), e (electron charge magnitude), k_{B} (the Boltzmann constant) as

$$c = 2.99792458 \times 10^8\,\mathrm{m/s} \approx 3.00 \times 10^8\,\mathrm{m/s}, \tag{1.9}$$

$$\hbar c = 197.326968\,\mathrm{MeV\,fm} \approx 200\,\mathrm{MeV\,fm}, \tag{1.10}$$

$$\frac{e^2}{\hbar c} = \frac{1}{137.035999074} \approx \frac{1}{137} \quad \text{(fine structure constant)}, \tag{1.11}$$

$$k_B T = 0.02482\,\mathrm{eV} \approx \frac{1}{40}\,\mathrm{eV} \text{ at } T = 288\,\mathrm{K}. \tag{1.12}$$

The quantity $e^2/\hbar c$ is called the fine structure constant. Equation (1.11) holds when the proportional coefficient in the static electric force between two particles with electric charge q_1, q_2 is determined such that the force is given by $F(r) = q_1 q_2 / r^2$ when the two particles are apart from each other by the distance r. Equation (1.12) represents the kinetic energy of thermal neutrons. It is useful to convert the temperature given in units of Kelvin to the corresponding energy in units of MeV.

Exercise 1.3 The range of force is given by the Compton wave length $\hbar/mc$ of the corresponding gauge particle. Estimate the range of the strong interaction and of the weak interaction.

Exercise 1.4 As Fig. 1.4 shows, the force between two protons is dominated by a repulsive Coulomb interaction at large distances, and turns attractive in the region inside their touching radius due to the nuclear force, i.e., due to the strong interaction. Estimate the height of the Coulomb barrier $V_{\mathrm{CB}} = V(r_B)$ by assuming that the touching radius is given by $r = r_B \sim 2 \times R_{\mathrm{p}} \sim 2\,\mathrm{fm}$, where R_{p} is the radius of the proton.

Exercise 1.5 The temperature of the Sun at the core is about 16 million K. Estimate the collision energy E at the core of the Sun.

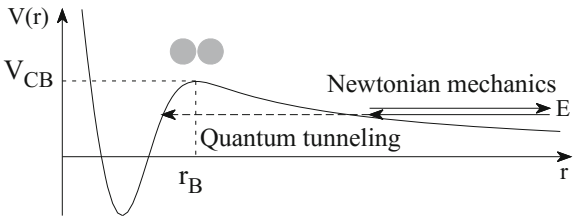

Fig. 1.4 Illustration of the collision between two protons in the Sun

Nuclear reactions in the Sun occur very slowly, because they take place by quantum tunneling as indicated by Exercises 1.4 and 1.5. In reality, there exists another important hindrance factor. As we learn later, there exists no stable bound state in the diproton system. The only stable dinucleon system is deuteron consisting of one proton and one neutron. In order for the fusion of two protons to take place, the inverse reaction of Eq. (1.8), where a proton is converted into a neutron by weak interaction, must therefore be involved. Because of the superposition of the quantum tunneling and weak interaction, the nuclear reaction between two protons is doubly hindered. Consequently, the Sun burns very slowly. It has burnt already for 4.6 billion years and is expected to continue to shine for another almost same period.

1.5 Species of Nuclei

The display of nuclei on the two-dimensional plane, where one axis, say the abscissa, represents the neutron number and the other, say the ordinate, the proton number, is called *Nuclear chart* or *Segré chart*. There are 256 stable nuclei if one includes those nuclei which have long lifetimes of the order comparable to the lifetime of the Sun such as U. They lie in the vicinity of the diagonal line of the nuclear chart for the reason we learn later. The reason why there exist more stable nuclei than the number of stable elements about 92 in nature is because there exist about three stable nuclei for each element on average. For example, there exist two stable nuclei, called proton p and deuteron d, for the element hydrogen.

Incidentally, the nuclei which have the same number of protons (i.e., the same atomic number), but differ in the neutron number, hence in the mass number as well, are called *isotopes* to each other, and those whose neutron numbers are the same, but the proton numbers are different, the *isotones*, and those which have same mass numbers the *isobars*, respectively.

The study of unstable nuclei with short lifetimes is currently one of the hot subjects of nuclear physics. If one includes unstable nuclei whose lifetime is longer than 1 μs, about 7000 nuclei are theoretically predicted to exist, among which about 3000 nuclei have already been discovered experimentally. Also, a group of nuclei stabilized by shell effects (see Chap. 5) are predicted to exist in the region far beyond U. They are called *superheavy nuclei* or *superheavy elements*, on which extensive studies are going on both experimentally and theoretically.

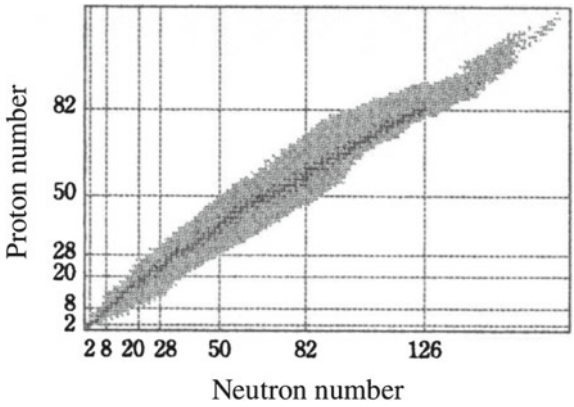

Fig. 1.5 Nuclear chart. Made from the 2010 version of Japan Atomic Energy Agency (JAEA)

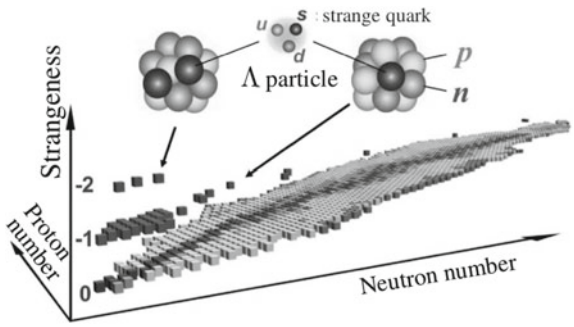

Fig. 1.6 Three-dimensional nuclear chart. Made by the experimental group of nuclear physics in the graduate school of science of Tohoku University

This book deals with nuclei made from the first-generation quarks, i.e., u and d quarks, from the point of view of the quark model. In recent years, however, nuclei containing Λ or Σ or Ξ particles, which include one or two second-generation s quark (s) as constituents, are also under extensive studies. These novel nuclei are called *hypernuclei*. A big progress of their study is expected to be stimulated by the operation of, e.g., J-PARC. Figure 1.5 shows the ordinary nuclear chart, while Fig. 1.6 a multi-layers nuclear chart, where the ordinate represents the strangeness number. The numbers appearing in Fig. 1.5 are the magic numbers, which we learn in Chap. 5.

To end this chapter, we mention the abundance of elements. Figure 1.7 shows the relative abundance of elements[5] in the conventional unit, i.e., by taking the abundance

[5] See also [4], where the relative abundance of even–even nuclear species with $A \geq 50$ in the solar system is given.

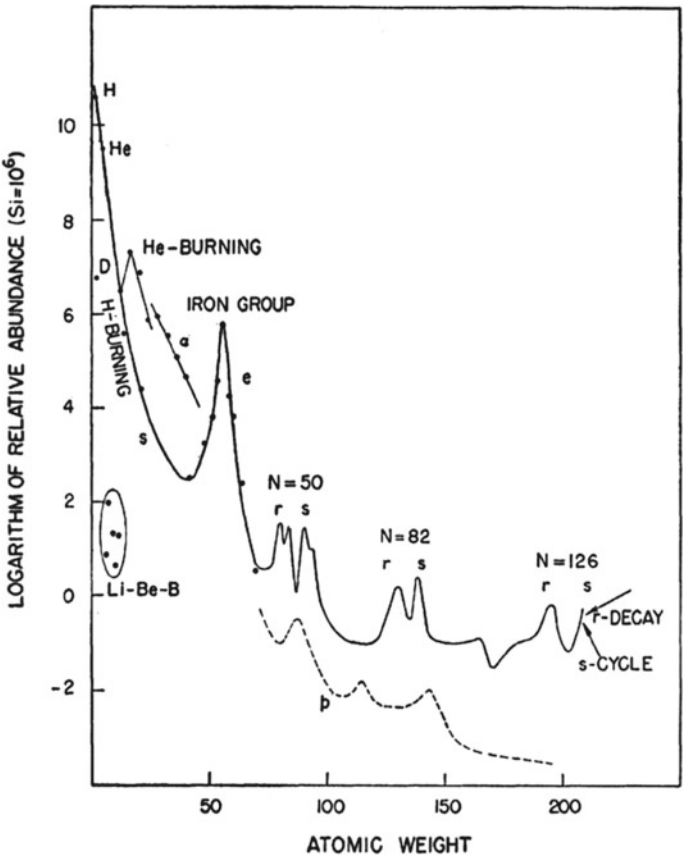

Fig. 1.7 Schematic curve of atomic abundances as a function of atomic weight based on the data of Suess and Urey [2]. Taken from [3]

of Si to be 10^6, i.e., H(Si) $= 10^6$. The hydrogen dominates by far, and the general trend is that the abundance sharply decreases with increasing mass number up to $A \sim 100$, then decreases much more slowly. In addition, it is noticeable that there appears a sharp peak of Fe group and that the abundances of nuclei with particular neutron numbers are large. Also, one notices that each of the latter abundances has twin peaks. These features originate from the stability of nuclei, and the magic numbers, and the way of nucleosynthesis. We will gradually learn them in this book.

1.6 Column: QCD Phase Diagram of Nuclear Matter

Water changes its state from ice (*solid phase*) to water (*liquid phase*), then to vapour (*gas phase*) when the temperature and the pressure vary. Similarly, nuclear matter changes its state or phase with temperature and density.

Figure 1.8 conceptually represents the phase diagram of nuclear matter from the point of view of QCD by taking the temperature and the chemical potential, which corresponds to the baryon density, for the ordinate and the abscissa, respectively. The region marked as nuclear matter is the state of nucleus treated in detail in this book.

As the figure shows, it is conjectured that a phase of quark–gluon plasma is achieved irrespective of the density if the temperature becomes high. Related experimental as well as theoretical studies are extensively performed including the high-energy heavy-ion collisions (Au + Au) using the RHIC (Relativistic Heavy Ion Collider) at the Brookhaven National Laboratory (BNL) in USA, and the Pb + Pb Collision experiments by the Large Hadron Collider (LHC) at the European Organization for Nuclear Research (CERN). The stars and the arrows in the diagram indicate the regions expected to be achieved by collision experiments and the expected paths of time evolution, respectively. There still remain, however, many uncertainties, including the phase diagram itself, and studies from various aspects are under way.

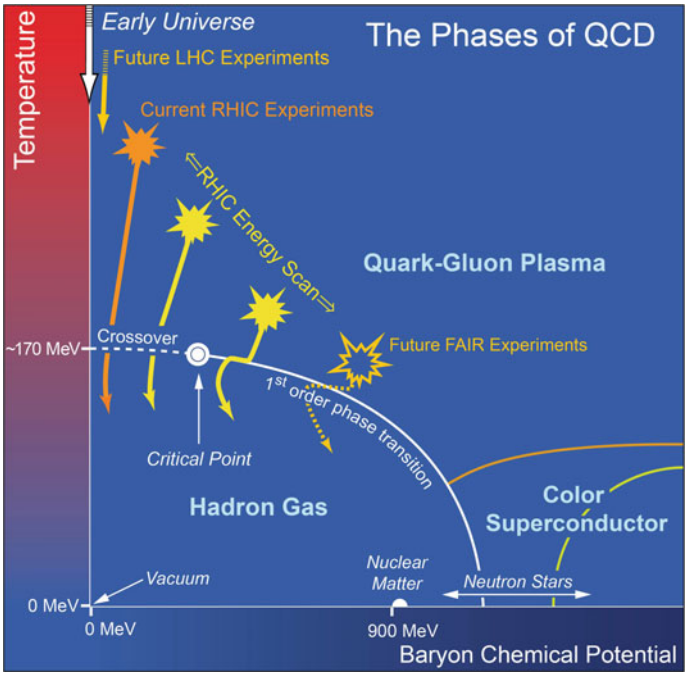

Fig. 1.8 QCD phase diagram. Taken from [5], courtesy of Brookhaven National Laboratory

References

1. W.-M. Yao et al. (Particle Data Group), J. Phys. G **33**, 1 (2006)
2. H.E. Suess, H.C. Urey, Rev. Mod. Phys. **28**, 53 (1956)
3. E.M. Burbidge, G.R. Burbidge, W.A. Fowler, F. Hoyle, Rev. Mod. Phys. **29**, 547 (1957)
4. Aage Bohr, Ben R. Mottelson, *Nuclear Structure*, vol. I (Benjamin, New York, 1969)
5. The Nuclear Science Advisory Committee, The Frontiers of Nuclear Science – A Long Range Plan (2007). http://science.energy.gov/np/nsac/

Chapter 2
Bulk Properties of Nuclei

Abstract Their sizes and masses are the most fundamental properties of nuclei. They have simple mass number dependences which suggest that the nucleus behaves like a liquid and lead to the liquid-drop model for the nucleus. In this chapter we learn these bulk properties of nuclei and their applications to discussing nuclear stability, muon-catalysed fusion and the structure of heavy stars. As an example of the applications we discuss somewhat in detail the basic features of fission and nuclear reactors. We also mention deviations from what are expected from the liquid-drop model which suggest the pairing correlation and shell effects. We also discuss the velocity and the density distributions of nucleons inside a nucleus.

2.1 Nuclear Sizes

2.1.1 Rutherford Scattering

At the beginning of the twentieth century when quantum mechanics was born, various models were proposed for the structure of atoms such as the *plum pudding* or *raisin bread model* of J.J. Thompson, which assumes that the plus charge distributes over whole atom together with electrons, and the *Saturn model* by Hantaro Nagaoka. Rutherford led these debates to conclusion through the study of scattering of alpha particles on atom. He proposed the existence of a central part of the atom, i.e., the core part, which bears all the positive charge that cancels out the total negative charge of electrons and also carries the dominant part of the mass of the atom. Rutherford named this core part nucleus, and gave the limiting value to its size.[1] At that time, Rutherford had been engaged in the detailed studies of the properties of alpha particles emitted from radioactive materials, and knew that the alpha particle is the ionized He. What Rutherford remarked in the experimental results of Marsden is that alpha

[1]It was 1911 when Rutherford submitted his article on the atomic model to a science journal. The idea and the formula of Rutherford were derived by stimulation of experimental results of his coworker Marsden who had been engaged in the study of scattering of alpha particles emitted from natural radioactive elements on matter. Furthermore, they have been confirmed experimentally to be correct by his collaborators Geiger and Marsden.

N. Takigawa and K. Washiyama, *Fundamentals of Nuclear Physics*,
DOI 10.1007/978-4-431-55378-6_2

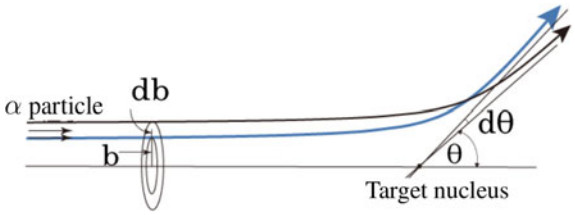

Fig. 2.1 Connection between the classical orbits of the Rutherford scattering and differential cross section

particles passing through matter sometimes make a large angle scattering, although most of them go nearly straight. This experimental feature cannot be explained by the Thompson model which assumes that positive charges distribute over the whole atom.[2]

It is established today that alpha particle is the nucleus of He. Here, we learn how the Rutherford model for atom was born, and how the information on the nuclear size is obtained through the scattering experiments of alpha particles.

Let us now consider the scattering of two structureless charged particles by Coulomb interaction, which is called Coulomb scattering or Rutherford scattering. Here, the two charged particles represent the alpha particle and the nucleus of the target atom. Since the mass of electrons is extremely small, one can ignore the scattering by electrons. The correct expression of the differential cross section for the Coulomb scattering can be obtained by classical mechanics, although, correctly speaking, one should use quantum mechanics. One important thing in this connection is that one to one correspondence holds between the impact parameter b and the scattering angle θ as illustrated in Fig. 2.1. The alpha particles which pass the area $2\pi b\mathrm{d}b$ of the impact parameter between b and $b + \mathrm{d}b$ in Fig. 2.1 are scattered to the region of solid angle $\mathrm{d}\Omega = 2\pi \sin\theta d\theta$ around the scattering angle θ. On the other hand, the differential cross section is defined as the number of particles scattered to the region of solid angle $\mathrm{d}\Omega$ when there exists one incident particle per unit time and unit area. Hence by definition

$$\frac{\mathrm{d}\sigma}{\mathrm{d}\theta} = \frac{2\pi b}{|\mathrm{d}\theta/\mathrm{d}b|}\,. \tag{2.1}$$

Using the relation

$$b = a\cot\left(\frac{\theta}{2}\right) \tag{2.2}$$

with

$$a = \frac{Z_1 Z_2 e^2}{\mu v^2} \tag{2.3}$$

[2]The history of the progress and discoveries of modern physics in the period from late in the nineteenth century to the beginning of the twentieth century is vividly described in the book by E. Segré [1].

which holds between the impact parameter b and the scattering angle θ in the case of Coulomb scattering, we obtain

$$\frac{\mathrm{d}\sigma}{\mathrm{d}\Omega} = \frac{\mathrm{d}\sigma_{\mathrm{R}}}{\mathrm{d}\Omega} \equiv \frac{1}{2\pi \sin\theta} \frac{\mathrm{d}\sigma}{\mathrm{d}\theta} = \frac{a^2}{4} \frac{1}{\sin^4(\theta/2)}, \tag{2.4}$$

where the index R in σ_{R} means the Rutherford scattering. In Eq. (2.3), μ is the reduced mass, and v is the speed of the relative motion in the asymptotic region, i.e., at the beginning of scattering. Note that Eq. (2.4) exactly agrees with the formula of the differential cross section $\mathrm{d}\sigma_{\mathrm{R}}/\mathrm{d}\Omega$ obtained quantum mechanically for the Rutherford scattering. The characteristics of the Coulomb scattering given by Eq. (2.4) are that the forward scattering is strong, but also that backward scattering takes place with a certain probability as well. These match the experimental results of Marsden.

The ground state of the natural radioactive nucleus $^{210}_{84}\mathrm{Po}$ decays with the half-life of 138.4 days by emitting an alpha particle ($^{210}_{84}\mathrm{Po} \rightarrow {}^{206}_{82}\mathrm{Pb} + \alpha$). The kinetic energy of the alpha particle is about 5.3 MeV corresponding to the Q-value of the decay 5.4 MeV. The differential cross section for the scattering, where this α particle is used to bombard the Au target of atomic number 79, agrees with that for the Rutherford scattering right up to the backward angle $\theta = \pi$. This suggests that the sum of the radii of Au and α ($R(\mathrm{Au}) + R(\alpha)$) is smaller than the distance of closest approach $d(\theta = \pi)$ for the scattering with the impact parameter $b = 0$ leading to the backward scattering $\theta = 180^\circ$ in the case of Rutherford scattering. Since the distance of closest approach d and the scattering angle θ or the impact parameter b is related by

$$d = a\left[1 + \csc\left(\frac{\theta}{2}\right)\right] = a + \sqrt{a^2 + b^2} \tag{2.5}$$

for the Rutherford scattering, the above mentioned experimental results give the upper boundary of the radius as $R(\mathrm{Au}) + R(\alpha) < 4.3 \times 10^{-12}$ cm. This upper boundary is much smaller than the radii of atoms, which are of the order of 10^{-8} cm. Rutherford was thus guided to his atomic model.

Figure 2.2 shows the ratio of the experimental differential cross section for the scattering of α particles of 48.2 MeV by Pb target to that for the corresponding Rutherford scattering $\mathrm{d}\sigma_{\mathrm{R}}/\mathrm{d}\Omega$ as a function of the scattering angle. The experimental cross section gets rapidly smaller than that of the Rutherford scattering beyond $\theta = 30^\circ$. This can be understood as the consequence of that the distance of closest approach is small for the scattering corresponding to large angle scattering as Eq. (2.5) shows, and hence the overlap between α particle and Pb becomes large, and consequently, those phenomena such as inelastic scattering which are excluded in the Rutherford scattering take place. Figure 2.3 shows classical trajectories obtained by fixing Pb at the origin and by making the incident energy of α particles to 48.2 MeV so as to match with Fig. 2.2. The circle shows the region corresponding to the sum of the radii of Pb and α particle, i.e., about 9.1 fm. The figure confirms that the distance of closest approach for the trajectories corresponding to large angle scattering becomes indeed smaller than the sum of the radii of Pb and α particle.

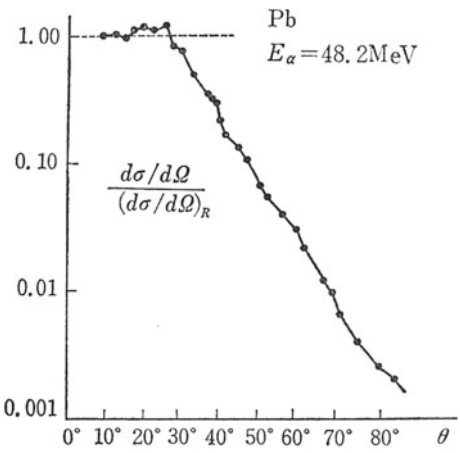

Fig. 2.2 Differential cross section of the elastic scattering of α particles by Pb. Taken from [2]

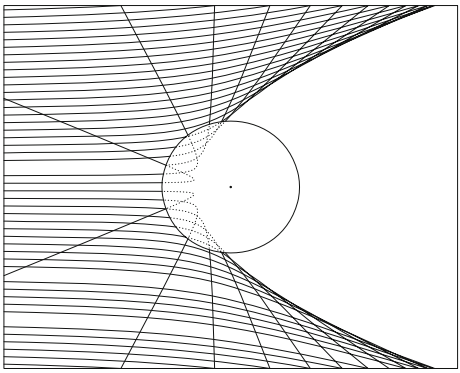

Fig. 2.3 Trajectories of Rutherford scattering

Exercise 2.1 Estimate the sum of the radii of α and Pb from the result of Fig. 2.2 based on the idea mentioned above.

The ratio of the differential cross section shown in Fig. 2.2 resembles the Fresnel diffraction of classical optics. The Fresnel diffraction occurs in the case where the source of light is located in the vicinity of the object that causes diffraction, e.g., an absorber. The scattering of α particles by a nucleus with large atomic number behaves like a Fresnel scattering, because the large Coulomb repulsion strongly bends the trajectory and works to make the source of light effectively locate in the vicinity of the scatterer. It is also because the partial waves corresponding to small impact parameters whose distance of closest approach is small are removed from the elastic scattering due to, e.g., inelastic scattering. Concerning the elastic scattering, this plays effectively the same role as that of an absorber.

This picture holds when the Coulomb interaction dominates the scattering process. The strength of the Coulomb interaction increases in proportion to the product of the charges of the projectile and target nuclei. On the other hand, roughly speaking,

the strength of the nuclear interaction increases in proportion to the reduced mass $A_1A_2/(A_1 + A_2)$. Hence the refraction effect due to the nuclear interaction becomes non-negligible for the scattering by a target nucleus with small atomic number. In fact, a similar differential cross section appears not by diffraction effect, but by refraction effect. The interpretation and analysis then get complicated. Accordingly, one can safely estimate the nuclear size based on the consideration of the Coulomb trajectory together with the strong absorption due to inelastic scattering as described in the present section when the atomic number of the target nucleus is large.

2.1.2 Electron Scattering

The scattering of α particles by a nucleus had led to the Rutherford atomic model, and provided a way to estimate the nuclear size. It thus played an important historical role. However, as stated at the end of the last section, it has a limitation regarding applicability. In contrast, the scattering of electrons by a nucleus, which we learn in this section, is a powerful method to study the nuclear size, more exactly, the distribution of protons inside a nucleus, because only well understood electromagnetic force is involved.[3,4]

2.1.2.1 The de Broglie Wavelength of Electron

In the experiments of electron scattering, electrons are injected on the target nucleus after they are accelerated by, e.g., a linear accelerator. In order to deduce the information on the nuclear size from electron scattering, the de Broglie wavelength of the electron must be of the same order of magnitude as that of the nuclear size or smaller. In this connection, let us first study the relation between the de Broglie wavelength of electron and the kinetic energy of electron supplied by the accelerator.

The de Broglie wavelength of electron λ_e is given by

$$\lambda_e = \frac{h}{p_e} \tag{2.6}$$

in terms of the momentum of the electron p_e and the Planck constant h. On the other hand, it holds that

$$E_{\text{total}} = \sqrt{m_e^2c^4 + p_e^2c^2} = m_ec^2 + E_{\text{kin}} = m_ec^2 + E_e \tag{2.7}$$

[3] R. Hofstadter was awarded the Nobel Prize in Physics 1961 for the study of high energy electron scattering with linear accelerator and the discovery of the structure of nucleon. He performed also systematic studies of nuclei by electron scattering.

[4] The electron scattering is a powerful method to learn the structure of nucleons mentioned in Chap. 1, and also to study nuclear excitations such as *giant resonances* and hypernuclei as well.

Table 2.1 The de Broglie wavelength of electron for some representative acceleration energies

Acceleration energy E_e (MeV)	100	200	300	1000	4000
de Broglie wavelength λ_e (fm)	12.4	6.2	4.1	1.2	0.31

by using the relation of relativity between the momentum and the energy of an electron, since the total energy of electron is given by adding the energy E_e supplied by the accelerator, i.e., the kinetic energy E_{kin}, to the rest energy. Hence,

$$p_e^2 = 2m_e E_e + E_e^2/c^2 \,. \tag{2.8}$$

By inserting Eq. (2.8) into (2.6), we obtain

$$\frac{\lambda_e}{2\pi} = \frac{\hbar c}{E_e(1 + 2m_e c^2/E_e)^{1/2}} \approx \frac{\hbar c}{E_e} \approx \frac{200}{E_e/\mathrm{MeV}}\,\mathrm{fm}\,. \tag{2.9}$$

We ignored the rest energy of electron $m_e c^2$ in the third and fourth terms of Eq. (2.9) by assuming that it is much smaller than the acceleration energy E_e. We have given not the wavelength itself, but the quantity which is obtained by dividing the wavelength by 2π to facilitate the estimate of the order of magnitude.

Table 2.1 gives the de Broglie wavelength of electron estimated by Eq. (2.9) for some representative acceleration energies.

2.1.2.2 Form Factor

As Table 2.1 shows, one has to inject electrons on a nucleus after having accelerated them to much higher energy than the rest energy of electron $m_e c^2 \approx 0.51\,\mathrm{MeV}$ in order to learn the nuclear size, which is of the order of fm. Hence one needs to use the Dirac equation, to which a relativistic Fermi particle obeys, in order to theoretically derive the proper expression of the differential cross section [3].

Exercise 2.2 Evaluate the ratio v/c of the velocity of the electron v to the speed of light in the vacuum c when the acceleration energy of the electron E_e is 100 MeV.

However, here let us simplify the problem in the following way, and learn how the information on nuclei can be obtained from the analyses of the electron scattering:

1. Treat the scattering of electrons by the electromagnetic field made by a nucleus, instead of considering the scattering of electrons by the nucleons inside the nucleus.
2. Consider only the Coulomb force (electric force) and ignore the magnetic force.
3. Use non-relativistic Schrödinger equation.

We express the Coulomb potential as $V(\mathbf{r})$. The scattering amplitude to the angle θ is then given by

$$f^{(1)}(\theta) = -\frac{1}{4\pi}\frac{2\mu}{\hbar^2}\int \mathrm{e}^{-\mathrm{i}\mathbf{q}\cdot\mathbf{r}} V(\mathbf{r})\mathrm{d}\mathbf{r} \tag{2.10}$$

following the first order Born approximation, which is valid because of the high energy scattering, and also because the involved electric force is weak compared to the kinetic energy. The μ is the reduced mass. It can be identified with the mass of electron m_e to a high degree of accuracy. The $\mathbf{q}$ is the momentum transfer divided by $\hbar$ and is given by

$$\mathbf{q} = \mathbf{k}_\mathrm{f} - \mathbf{k}_\mathrm{i}\,, \tag{2.11}$$

$$q = |\mathbf{q}| = 2k\sin(\theta/2)\,. \tag{2.12}$$

where $\mathbf{k}_\mathrm{i}$ is the wave-vector of the incident electron, $\mathbf{k}_\mathrm{f}$ is the wave-vector of the electron scattered to the direction of angle θ and k is the wave number of the electron corresponding to the incident energy.

Exercise 2.3 Derive Eqs. (2.10)–(2.12).

We remark that the potential $V(\mathbf{r})$ obeys the following Poisson equation,

$$\Delta V = 4\pi Ze^2\rho_C(\mathbf{r})\,, \tag{2.13}$$

in order to relate the scattering amplitude to the distribution of protons inside a nucleus. The Z is the atomic number of the nucleus to be studied, and $\rho_C(\mathbf{r})$ is the charge density at the position $\mathbf{r}$ measured from the center of the nucleus.[5] It is normalized as

$$\int \rho_C(\mathbf{r})\mathrm{d}\mathbf{r} = 1\,. \tag{2.14}$$

By repeating the integration by parts twice in Eq. (2.10), and by using Eq. (2.13), we obtain,

$$f^{(1)}(\theta) = \frac{Ze^2}{2\mu v^2}\frac{1}{\sin^2(\theta/2)}F(\mathbf{q})\,, \tag{2.15}$$

where $F(\mathbf{q})$ is defined as

$$F(\mathbf{q}) \equiv \int \mathrm{e}^{-\mathrm{i}\mathbf{q}\cdot\mathbf{r}}\rho_C(\mathbf{r})\mathrm{d}\mathbf{r}\,. \tag{2.16}$$

The differential cross section is therefore given by

$$\frac{d\sigma^{(1)}}{d\Omega} = |f^{(1)}(\theta)|^2 = \frac{d\sigma_\mathrm{R}}{d\Omega}|F(\mathbf{q})|^2\,. \tag{2.17}$$

[5] The distribution of protons ρ_p can be derived from ρ_C by taking into account the intrinsic structure of proton.

Correctly, the expression of the differential cross section is obtained as

$$\frac{\mathrm{d}\sigma^{(1)}}{\mathrm{d}\Omega} = \frac{\mathrm{d}\sigma_{\mathrm{M}}}{\mathrm{d}\Omega}|F(\mathbf{q})|^2 , \tag{2.18}$$

$$\frac{\mathrm{d}\sigma_{\mathrm{M}}}{\mathrm{d}\Omega} = \left[\frac{Ze^2}{2E_{\mathrm{e}}\sin^2(\theta/2)}\right]^2 \left[1 - \frac{v^2}{c^2}\sin^2(\theta/2)\right]$$

$$\approx \left[\frac{Ze^2\cos(\theta/2)}{2E_{\mathrm{e}}\sin^2(\theta/2)}\right]^2 , \tag{2.19}$$

by replacing the differential cross section of the Rutherford scattering $\mathrm{d}\sigma_{\mathrm{R}}/\mathrm{d}\Omega$ by that for the Mott scattering $\mathrm{d}\sigma_{\mathrm{M}}/\mathrm{d}\Omega$ which takes into account relativistic effects for electrons. The $\mathrm{d}\sigma_{\mathrm{M}}/\mathrm{d}\Omega$ gives the differential cross section of the scattering of electrons by the Coulomb force made by a point charge. Equation (2.18) shows that the information on the density distribution of protons inside a nucleus can be obtained through the ratio of the experimental differential cross section to that for the Mott scattering. The $F(\mathbf{q})$ defined by Eq. (2.16) is the factor which represents the effects of the finiteness of the nuclear size and is called the *form factor*.

Especially, if the nucleus is spherical, i.e., if the charge distribution is spherical, the form factor is given by

$$F(q) = 4\pi \int_0^\infty \rho_C(r) j_0(qr) r^2 \mathrm{d}r = 4\pi \int_0^\infty \rho_C(r) \frac{\sin(qr)}{qr} r^2 \mathrm{d}r , \tag{2.20}$$

where $j_0(x)$ is the spherical Bessel function of the first kind.

Exercise 2.4 Prove Eq. (2.20) in the following two methods:

1. Perform directly the integration over the angular part of $\mathbf{r}$ ($\mathrm{d}\Omega_r$) in Eq. (2.16).
2. Expand at first the $\mathrm{e}^{-\mathrm{i}\mathbf{q}\cdot\mathbf{r}}$ in terms of Legendre functions, and then use the orthonormal property of the spherical harmonics.

2.1.2.3 Density Distribution

(1) Estimate of the Nuclear Radius from Diffraction Pattern As Table 2.1 implies, the experiments of electron scattering are performed with high energy in order to study nuclear size and the density distribution of protons inside a nucleus. The corresponding differential cross section is expected to show a diffraction pattern similar to that of the Fraunhofer diffraction in optics. Figure 2.4 shows the differential cross section for the elastic scattering of electrons from Au target at 153 and 183 MeV. The monotonically decreasing solid line is the Mott scattering cross section for 183 MeV. The figure shows that the observed cross section is smaller than that for the Mott scattering, and that it has indeed the diffraction pattern, i.e., oscillation, of the Fraunhofer type.

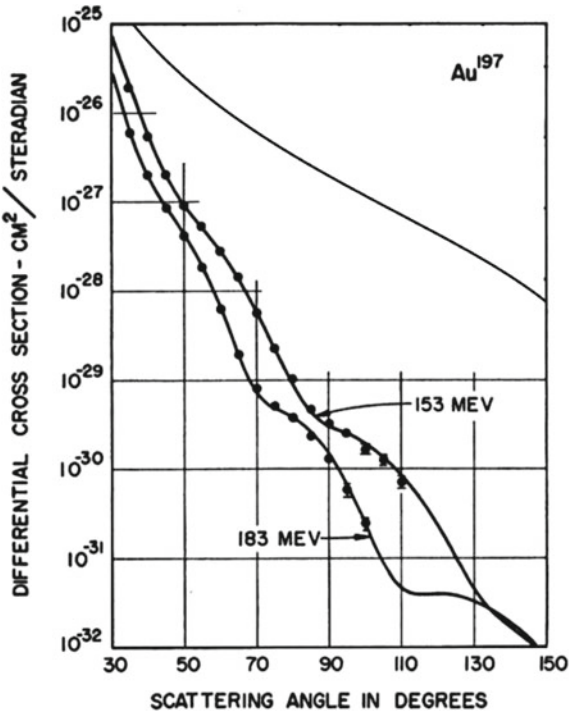

Fig. 2.4 The elastic electron-scattering differential cross section from Au at energies of 153 and 183 MeV. Taken from [4]

Let us assume that the charge distributes uniformly inside a nucleus with a spherical shape of radius R in order to see how the nuclear size is estimated from the diffraction pattern. The resulting form factor reads

$$F(q) = \frac{3}{qR} j_1(qR) = \frac{3}{qR}(qR)^{-2}[\sin(qR) - (qR)\cos(qR)]\,. \tag{2.21}$$

We then find that the zeros of $j_1(x)/x$ correspond to the angles where the differential cross section shows local minima. We denote the magnitude of the transferred momenta corresponding to those scattering angles $\theta_1, \theta_2, \ldots$ by $q_1, q_2, \ldots$. The first zero of $j_1(x)/x$ is $x_1 \approx 4.49$, and the interval between the successive zeros Δx is about π afterwards. One can therefore estimate the radius either by $R \sim x_1/q_1$ or by $R \sim \pi/(q_2 - q_1)$ using the $q_1, q_2, \ldots$ evaluated from $\theta_1, \theta_2, \ldots$, which are extracted from the experimental data.

Exercise 2.5 Estimate the radius of the nucleus of Au from the experimental data shown in Fig. 2.4.[6]

[6]The dips in diffraction pattern are buried by the distortion effects due to Coulomb force in the case of target nuclei with a large mass number such as Au. The diffraction pattern appears more clearly for the target nuclei with small mass number.

(2) The Woods–Saxon Representation of the Density Distribution Accurate information on the density distribution[7] of nucleons inside a nucleus can be obtained by making the Fourier transformation of the form factor given by the experiments of electron scattering. However, one usually takes the method to first postulate a plausible functional form, then determine the parameters therein to reproduce the experimental data. In that case, a widely adopted choice is to assume the following functional form called the *Woods–Saxon type*,[8]

$$\rho(r) = \frac{\rho_0}{1 + \mathrm{e}^{(r-R)/a}}\,, \tag{2.22}$$

where R is the parameter to represent the radius. a is the parameter to represent the thickness of the surface area and is called the surface diffuseness parameter. The density falls from 90 to 10% of the central density over the region of thickness of 4.4 times a around R. The ρ_0 is the central density, and is given as a function of R and a through the normalization condition,

$$\int \rho \mathrm{d}\mathbf{r} \sim \rho_0 \frac{4\pi}{3} R^3 \left[1 + \pi^2 \left(\frac{a}{R}\right)^2\right] = A\,. \tag{2.23}$$

The two solid curves in Fig. 2.4 which reproduce fairly well the experimental differential cross section have been calculated with the best fit parameters for the data at 183 MeV by assuming the Woods–Saxon representation for the charge distribution.

The following values are obtained from the analyses of experimental data for a large number of stable target nuclei,

$$R \sim (1.1\text{–}1.2) A^{1/3}\,\mathrm{fm}\,, \quad a \sim 0.6\,\mathrm{fm}\,, \quad \rho_0 \sim (0.14\text{–}0.17)\,\mathrm{fm}^{-3}\,, \tag{2.24}$$

as parameters in the Woods–Saxon parametrization.[9] The fact that the radius is proportional to the 1/3 power of the mass number, i.e., the number of nucleons composing the nucleus, and that the density is independent of the mass number

[7] In stable nuclei, the protons and neutrons distribute inside the nucleus almost in the same way. Here, we therefore treat the density distribution of protons and of nucleons as the same except for the absolute value. In these days, extensive studies are performed on the nuclei far from the β-stability line, which are called unstable nuclei. It is then getting known that some of them have very different distributions for protons and for neutrons. For example, the region where there exists only neutrons largely extends over the surface region in some nuclei such as ^{11}Li in the vicinity of the neutron drip line. Such layer is called the *neutron halo*. Recently, it is reported from the inelastic scattering of polarized protons (see [5]) and also from the elastic scattering of polarized electrons that even a typical stable nucleus ^{208}Pb has a larger radius of the neutron distribution than that of the proton distribution by 0.15–0.33 fm. Relatedly, the study of the existence of the region consisting of only neutrons, which is called *neutron skin*, is an active area of research.

[8] There exist deviations from the Woods–Saxon type for individual nucleus. They are explained by shell model.

[9] The value $\rho_0 \sim 0.17\,\mathrm{fm}^{-3}$ is widely accepted as the density of nuclear matter (see [6] for the argument about the detailed mass number dependence of the central density of nuclei with large mass number).